Phase Modulation and Optical Anisotropy of High Birefringence Liquid Crystals

V. Urruchi [a] , I. Pérez [a] , N. Gaona [a] & J. M. Sánchez-Pena [a]

[a] Grupo de Displays y Aplicaciones Fotónicas; Dpto.
Tecnología Electrónica, Escuela Politécnica Superior,
Universidad Carlos III, Leganés, Madrid, Spain

PLEASE SCROLL DOWN FOR ARTICLE

for any loss, actions, claims, proceedings, demand, or costs or damages whatsoever or howsoever caused arising directly or indirectly in connection with or arising out of the use of this material.

Taylor & Francis
Taylor & Francis Group

Phase Modulation and Optical Anisotropy of High Birefringence Liquid Crystals

V. Urruchi, I. Pérez, N. Gaona, and J. M. Sánchez-Pena

Grupo de Displays y Aplicaciones Fotónicas; Dpto. Tecnología
Electrónica, Escuela Politécnica Superior, Universidad Carlos III,
Leganés, Madrid, Spain

Phase modulation and optical anisotropy of high birefringence liquid crystal mixtures are studied in this work. Phase measurements are performed via voltage dependent interferometric pattern shifts at a wavelength of 632.8 nm. Wavelength dependence of optical anisotropy is carried out by polarizing microscopy via transmittance spectra from 450 nm to 720 nm. Nematic liquids crystal mixtures are sandwiched between two glasses which are homogeneously aligned and assembled untwisted.

The results of phase shifts are compared to those of conventional nematic liquid crystals. It has been shown that high birefringence liquid crystals are potential candidates for generating phase shifts which are higher (∼6π) than those of conventional nematic liquid crystals (normally about 2π).

Keywords: birefringence; interference; optical microscopy; phase shift; spectral analysis

INTRODUCTION

Phase modulation of light is a significant characteristic in non-display applications such as coherent optical systems processing or diffractive optical elements in optical instruments. In particular, phase-only

modulation is desirable for laser applications and adaptive optics. Some proposals [1] for phase-only devices have reported excellent phase shifts.

The generation of phase modulation in liquid crystal devices is concerned with a set of causes. These dependences can arise from a physical property of the liquid crystal mixture (like the birefringence), or the mechanical arrangement of the device, or its particular switching mode. Usually the modulation is due to the combined effect of various factors. For example, vertical aligned nematic liquid crystals exhibit electrically controlled birefringence [2]: negative birefringence, together with a specific structure of homeotropic alignment, induces adaptative phase retardations in a controlled mode.

Nematic liquid crystal mixtures, recently synthesized, are a promising opportunity for developing new devices with the generation of large phase delays and nearly phase-only modulation, with high birefringence being a key feature of these liquid crystals. On the other hand, the homogeneous alignment of the molecules inside the sandwich, together with the parallel arrangement of the glasses, requires fabrication processes which are not excessively complex. Hence, devices with this type of configuration have been considered in this work. The propagation of polarized light in untwisted nematic liquid crystal devices is well-known in literature [3]. The phase delay of these devices depends on some basic parameters such as birefringence, cell thickness, wavelength of the incident light or external voltage. In the analysis, experimental nematic liquid crystal mixtures of high birefringence have been chosen to fill the devices. This feature makes them potential candidates for generating phase delays which are higher than those of conventional nematic liquid crystals (normally about 2π).

Reported methods deal with the characterization of the *phase modulation* and the *amplitude modulation*. On the one hand, some reported procedures have been implemented in the past to explore the behavior of the phase shift, many of them based on interferometry [4–6]. In this work, a set of devices have been evaluated to characterize the *phase modulation* using an interferometric technique. On the other hand, the wavelength dependence of the mixture birefringence, within a visible wavelength range, has been characterized. Spectral characterization uses mathematical tools similar to some techniques previously reported [7–12]. Those methods base the analysis on the *amplitude modulation* of light transmittance through the device. Changes of the transmittance have been measured by optical microscopy with polarized light placing the cell between crossed and parallel polarizers.

THEORETICAL DESCRIPTION OF MEASUREMENTS

Phase Shift Measurement by Interferometry

As two waves with the same state of linear polarization interfere, the formation of the interference pattern may be done with the assumption that the two waves are coherent. Then, the intensity of the interference can be written in a simplified expression,

$$I(x,y) = 2 \cdot I_0(x,y) \cdot [1 + \cos \delta(x,y)] \qquad (1)$$

where $I_0(x, y)$ is the intensity from both sources and $\delta(x, y)$ is the *phase difference* between the two waves.

The phase shifting method is based on the reconstruction of the *phase difference* by quantitative analysis of the fringe displacement (of the interference patterns). Concerning the devices of this work, in liquid crystal the voltage dependence of phase retardation is the key to phase shift generation.

As regards the interference intensity, it depends on a sinusoidal function characterized by periodic behavior. Thus, a direct measurement of the fringe displacement at each voltage can deliver the *phase shift*, $\Delta\delta'$, with an easy expression,

$$\Delta\delta' = \frac{\Delta x}{T} \cdot 2\pi \qquad (2)$$

with Δx being the displacement of the fringe and T the period of the fringe. However, this procedure does not recover the absolute phase at each voltage. Moreover, there is an ambiguity problem when the *phase shift* is higher than 2π. The value of the continuous *phase shift* must be obtained removing all the phase discontinuities every 2π. This method requires establishing a phase reference point and having additional information from the device to distinguish the increasing or decreasing phase evolution. Hence, the continuous *phase shift*, $\Delta\delta$, can be expressed as

$$\Delta\delta = \Delta\delta' \pm N \cdot 2\pi \qquad (3)$$

where $\Delta\delta'$ is the phase modulo 2π previously considered and N is the integer fringe number [13].

For untwisted nematic liquid crystals with positive birefringence, it is well-known that switching forces the molecules to tilt gradually as a voltage is applied to the device. Thus, the assumption that normal incident light experiences the refractive index n_e, at the lowest voltages, and n_o, at the highest voltages, may be made neglecting

the effects of the two thin layers of liquid crystal on top of the glasses. Using that hypothesis, the total *phase shift* measured with an interferometer is given by the equation,

$$\Delta\delta = \delta(V_{Thr}) - \delta(V_{Ref}) \qquad (4)$$

The *phase difference* at V_{Ref} (reference voltage) and V_{Thr} (threshold voltage) are, respectively,

$$\delta(V_{Thr}) = \frac{2\pi}{\lambda} \cdot [n(V_{Thr}) \cdot d - (r_1 - r_2)] \qquad (5)$$

$$\delta(V_{Ref}) = \frac{2\pi}{\lambda} \cdot [n(V_{Ref}) \cdot d - (r_1 - r_2)] \qquad (6)$$

where $n(V_{Ref})$ and $n(V_{Thr})$ are the effective refractive indexes at those voltages, d is the cell gap and r_1–r_2 is the optical path difference of the two arms.

Finally, the total *phase shift* is,

$$\Delta\delta = \frac{2\pi}{\lambda} \cdot [n(V_{Thr}) - n(V_{Ref})] \cdot d = \frac{2\pi}{\lambda} \cdot [n_e - n_o] \cdot d = \frac{2\pi \cdot \Delta nd}{\lambda} = \varphi \quad (7)$$

That is, the total *phase shift* at the extreme voltages of the interval is like the *phase retardation* that an electric field, linearly polarized along one axis, would experience traveling through a medium with variable refractive index along that axis. The extreme values of the refractive index would be n_e and n_o.

Intensity Measurement by Polarizing Microscopy

The expressions of the intensities between crossed and parallel polarizers passing through homogeneous untwisted nematic liquid crystal devices, $I_\perp$ and $I_\parallel$, respectively, depend on the *phase retardation*, φ, as

$$I_\perp = I_0 \sin^2 2\alpha \cdot \sin^2 \frac{\varphi}{2} \qquad (8)$$

$$I_\parallel = I_0 \cdot \left(1 - \sin^2 2\alpha \cdot \sin^2 \frac{\varphi}{2}\right) \qquad (9)$$

with

$$\varphi = \frac{2\pi \cdot \Delta nd}{\lambda} \qquad (10)$$

I_0 is the intensity of the incident light, α is the angle between the liquid crystal director and the optical axis of the first polarizer, Δn the birefringence, d the cell gap and λ the wavelength. The intensities reach the maximum and the minimum values as α is $\pi/4$.

In materials with positive birefringence, as those considered in this work, the phase retardation φ, is positive and the *effective* birefringence decreases as the voltage between the cell electrodes increases.

Using $\alpha = \pi/4$ in Eqs. (8) and (9), the *phase retardation φ* is obtained, at every wavelength, as

$$\varphi = \begin{cases} N \cdot \pi + \arccos\left(\frac{I_{\parallel}-I_{\perp}}{I_{\parallel}+I_{\perp}}\right) & N = 0, 2, 4, \ldots \\ (N+1) \cdot \pi - \arccos\left(\frac{I_{\parallel}-I_{\perp}}{I_{\parallel}+I_{\perp}}\right) & N = 1, 3, 5, \ldots \end{cases} \quad (11)$$

This calculation recovers the absolute value of the phase. The value of N can be inferred by analyzing the switching conditions of the liquid crystal device and the birefringence can be immediately deduced from the phase.

In the same way a systematic calculation can be repeated by selecting a set of individual wavelengths of the incident light within visible wavelength range.

EXPERIMENTAL SET-UP

An experimental nematic liquid crystal mixture synthesized by the Military University of Technology (MUT) in Warsaw with high birefringence ($\Delta n = 0.37$ at $\lambda = 633\,nm$) [13], has been chosen to fill the devices. The devices were monopixel cells with an active area of $0.5\,cm^2$, $5\,\mu m$ of thickness, homogeneous alignment and parallel arrangement of the glass substrates (untwisted). Driving schemes were square signals of $1\,kHz$ with variable amplitude from $0.1\,V_{rms}$ to $5.5\,V_{rms.}$

Interferometric Experimental Set-up

The experimental set-up is based on a Michelson interferometer architecture (Fig. 1).

A polarized He-Ne laser beam ($\lambda = 632.8\,nm$) was used as a light source. The laser beam strikes a beamsplitter which splits the incoming light into two optical beams: beam 1 propagates toward a mirror; the liquid crystal device is placed in the path of beam 2 toward a second mirror. The two beams reflected off of the mirrors
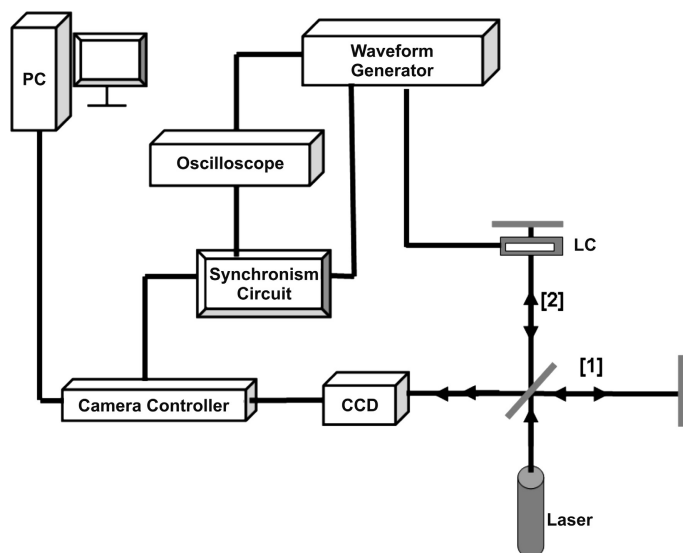
FIGURE 1 Arrangement of the components for the experimental set-up based on a Michelson interferometer architecture.

are recombined as they meet together at the beamsplitter, interfering with each other. The interference pattern reflected from the beamsplitter is recorded in a CCD camera. An external synchronism circuit has been designed to trigger the Hamamatsu Orca-AG CCD and to fix the times of image acquisition. The images have been treated with appropriate software in a PC.

In this scheme the interference pattern arises from the *phase difference*, δ, between the beams traveling through the two arms of the interferometer. The optical retardation in this particular configuration is on account of the effect of the liquid crystal refractive index at each applied voltage. Each fringe profile represents a distinctive feature of the device independently of the number of pattern fringes.

The experiments have been carried out with the cell placed in the path of beam 2 so that the direction of the liquid crystal molecules, for no voltage applied, was parallel ($\alpha = 0$) to the linearly polarized incoming light.

Experimental Set-Up Based on Polarizing Microscopy

Spectral responses have been measured placing the liquid crystal samples on the stage of a Nikon Eclipse E600 polarizing microscope with a 100 W tungsten-halide lamp. Cells have been placed between crossed

and parallel polarizers with the molecular director at $\pi/4$ from the linear polarization at the input.

An Acton Research Co. SpectraPro 300i monochromator, with a spectral range from 300 nm to 1000 nm, has been used to select every single wavelength of the lamp emission spectrum. The spectrograph output slit is assembled with a Hamamatsu photomultiplier tube controlled by a personal computer.

Finally, an optical fiber bundle was used to connect the microscope output to the monochromator input slit.

Optical transmissions have been acquired at the experimental wavelength interval from 450 nm to 720 nm. All measurements have been carried out at room temperature ($25°C$).

RESULTS AND DISCUSSION

This section reports the characterization results of phase modulation and optical anisotropy of the experimental high birefringence liquid crystal synthesized by MUT.

(A) Phase Modulation Measurements by Interferometry at 632.8 nm

The first results illustrate the behavior of the interference patterns. Each graph in Figure 2 corresponds to a set of interference fringes for an interval of $0.5\,V_{rms}$ of a square signal. Looking at the graphics, fringe displacements confirm the hypothesis foreseen by the theoretical switching of untwisted nematic liquid crystals. The lower the root mean square voltage, the higher the phase change. At the highest voltages the interference patterns do not move and superimpose one fringe onto another. As the voltage decreases the displacements are not uniform.

The behavior of the *phase shift* at each root mean square voltage is shown in Figure 3. The pattern near the saturation voltage has been considered as the reference pattern ($V_{Ref} = 5.5\,V_{rms}$). The fringe displacements are quantities relative to this reference position. The switching threshold voltage ($V_{Thr} = 0.6\,V_{rms}$) is the lower voltage considered; this phase is almost constant for lower values and significant phase changes happen for higher voltages. Notice that the absolute value of the phase is unknown but the zero phase reference in V_{Ref} is an acceptable assumption. The total *phase shift* accumulates 6.1π, from the reference voltage to the threshold voltage. Such a value is a very promising result since the experimental mixture generates higher phase retardation than those of conventional nematic liquid crystals.
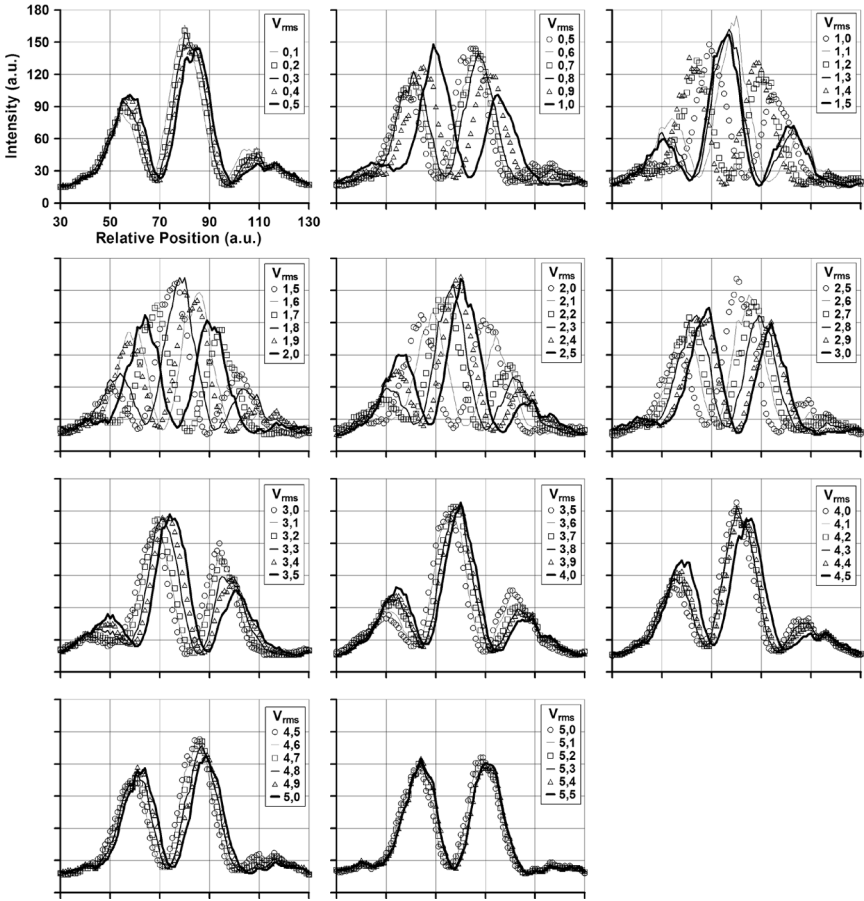
FIGURE 2 Interference patterns of a high birefringence nematic liquid crystal device, recorded in a CCD as a conventional square signal is applied.

The phase modulo 2π has been calculated using the Eq. (2) but dividing by two. The reason is that light travels through the liquid crystal cell twice in a Michelson interferometer. The total *phase shift* has been obtained by adding the corresponding integral multiples of 2π to the previous values from the reference.

(B) Spectral Response and Wavelength Dependence of the Birefringence

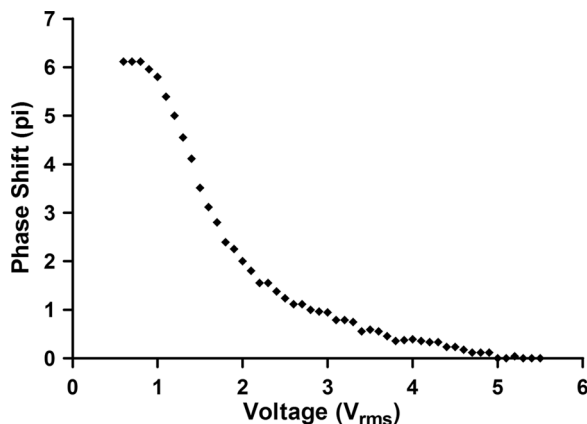Transmittances through the devices have been measured by optical microscopy.

FIGURE 3 Voltage dependence of the phase shift of a high birefringence nematic liquid crystal mixture at $\lambda = 632.8$ nm.
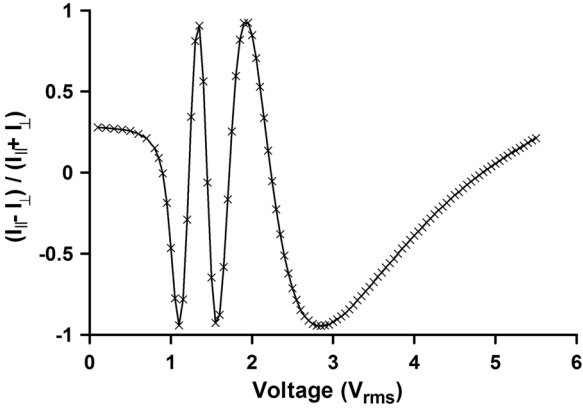
First, intensities between crossed and parallel polarizers were acquired at a fixed light wavelength and a range of voltages. The experimental results for the intensities and the dependence relation at 632.8 nm are graphed in Figures 4(a) and (b), respectively. The profiles of the intensities are the sources for deducing the number N. In this sense, if $I_\perp = I_\parallel$, the *arcos* becomes zero and the *phase shift* is $\pi/2$. Next, if $I_\perp$ reaches a maximum or $I_\parallel$ a minimum, the *phase shift* is consequently π. N = 0 at the first slope of the intensities from the highest voltages. N = 1 at the following slope, and successively so at lower voltages. The demodulation with the number N of the wrapped phase allows the delivery of a continuous *phase shift* with the absolute value of the phase.

The results show that the relation of Figure 4(b) is nearly constant, and the *phase shift* does not change any more at lower voltages than $0.6 \, V_{rms}$. The maximum *phase shift* is 5.58π, at this switching threshold voltage, which is roughly in agreement with that previously obtained with the interferometric measurement.

The birefringence is directly related to the total *phase shift* of the liquid crystal, using Eq. (7). Figure 5 graphs the voltage dependence of the *effective* birefringence. The dynamic range (10–90%) of the device is about $1.5 \, V_{rms}$. Moreover, intensity measurements deliver an experimental value of birefringence of the mixture, $\Delta n = 0.35$ at $\lambda = 632.8$ nm. This value is nearly in agreement with the reported value for the mixture.
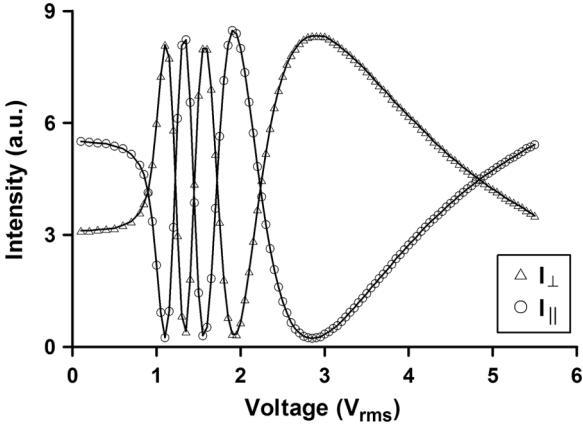
(a)

(b)

FIGURE 4 Voltage dependence of intensities between crossed and parallel polarizers of a high birefringence nematic liquid crystal mixture at $\lambda = 632.8$ nm. a) $I_\perp$ contrasted with $I_{||}$; b) Relation of dependence.

The same intensity measurements were carried out for a set of discrete wavelength values from 450 nm to 720 nm. Figure 6 displays the intensities between crossed polarizers at four particular wavelengths: 480 nm, 550 nm, 635 nm, and 700 nm, chosen from the measurements. All the intensities are normalized with regard to the microscope light source once the first polarizer is crossed. Inspecting the graphs, optical responses show a different number of maxima depending on the wavelength considered. The number of maxima decreases as the wavelength increases. While the number of maxima is directly related
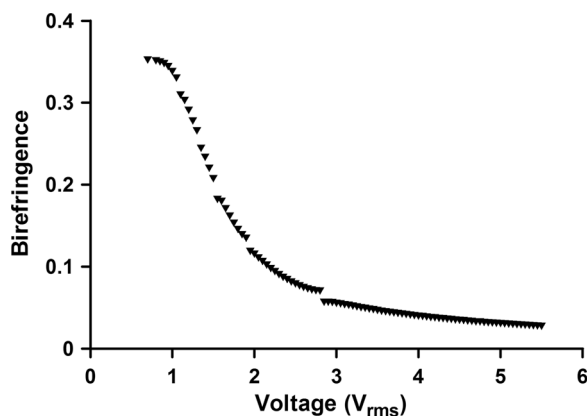
FIGURE 5 Voltage dependence of the effective birefringence of a high birefringence nematic liquid crystal mixture at $\lambda = 632.8$ nm.

to the total *phase shift*, as proved previously at $\lambda = 632.8$ nm, then, the higher the wavelength, the lower the total *phase shift*.

Finally, the wavelength dependence of the birefringence is shown in Figure 7. The result is a translation of the phase response: the higher the wavelength, the lower the birefringence. Birefringence of the liquid crystal mixture changes from 0.43 to 0.33 as the wavelength
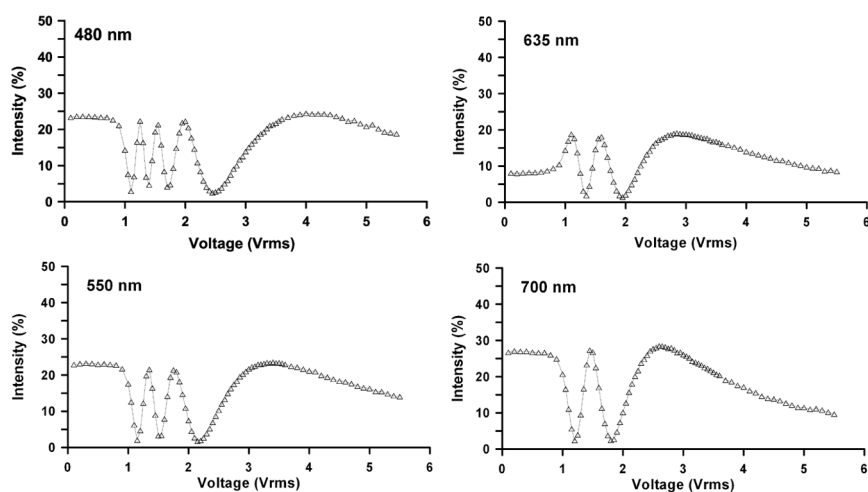

FIGURE 6 Voltage dependence of intensities between crossed polarizers of a high birefringence nematic liquid crystal sample at four source wavelengths.
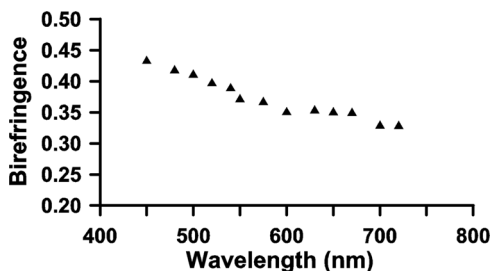
FIGURE 7 Wavelength dependence of the optical anisotropy of a high birefringence nematic liquid crystal device.

varies from 450 nm to 720 nm. This interval of birefringence corresponds to a *phase shift* range from 9.56π to 4.46π. The result reveals that a high phase change (5.1π) can be generated within a wavelength interval of 270 nm.

CONCLUSIONS

Characterization of phase modulation and optical anisotropy studies of homogeneous untwisted devices, filled with high birefringence mixtures, have been carried out. Phase, deduced from the interference pattern analysis, accumulates shifts of 6π at 632.8 nm. This value improves those of conventional nematic liquid crystal mixtures by about 2π and is roughly in agreement with that resulting from the intensity measurements.

Intensity measurements deliver an experimental value of the mixture birefringence, $\Delta n = 0.35$ at $\lambda = 632.8$ nm which is nearly in agreement with the reported value for the mixture supplied by the liquid crystal manufacturers. The spectral responses reveal that the higher the wavelength, the lower the total *phase shift* and the lower the birefringence, within a wavelength range from 450 nm to 720 nm. This result shows that a high phase change (5.1π) can be generated for a wavelength interval of 270 nm.

REFERENCES

[1] Yang, D-K. *et al.* (2006). *Fundamentals of Liquid Crystal Devices.*, Wiley: Chichester, UK.
[2] Lueder, E. (2001). *Liquid Crystal Displays. Addressing Schemes and Electro-Optical Effects*, Wiley: Chichester, UK.
[3] Pochi, Y. *et al.* (1999). *Optics of Liquid Crystal Displays*, Wiley: New York, USA.
[4] Hwang, S. J. (2005). *Journal of Display Technology*, **1**, 77.

[5] Urruchi, V., Gaona, N., & Sánchez-Pena, J. M. (2008). *Mol. Cryst. Liq. Cryst.*, *494*, 272. (in press).

[6] Wu, S-T., Efron, U., & Hess, L. D. (1984). *Appl. Optics.*, *23*, 3911.

[7] Benkelfat, B.-E., Horache, E.-H., Zou, Q., & Vinouze, B. (2003). *Opt. Commun.*, *221*, 271.

[8] San, S. E., Köysal, O., Özder, S., & Ecevit, F. N. (2003). *Turk. J. Phys.*, *27*, 279.

[9] Yusuf, Y., Sumisaki, Y., & Kai, S. (2003). *Chem. Phys. Lett.*, *382*, 198.

[10] Chang, H.-F., Chou, C., Teng, H.-K., Wu, H.-T., & Yau, H.-F. (2006). *Opt. Commun.*, *260*, 420.

[11] Ohkubo, K., Ohtsubo, J., & Izumi, N. (1994). *Appl. Optics*, *33*, 5895.

[12] Spadlo, A., Dąbrowski, R., Dziaduszek, J., Urban, S., Scibior, E., Gauza, S., & Wu, S.T. (2005). *Journal of Optical Technologies*, *72*, 659.

[13] Rastogi, P. K. (1997). *Optical Measurement Techniques and Applications*, Artech House: Boston, USA.